

Pyrolysis of 1,2-Ethanediol Monoacetate as Bifunctional Biofuel

Ahmed M. El-Nahas*, Islam M. Meligi, and Safinaz H. El-Demerdash

Chemistry Department, Faculty of Science, Menoufia University, Shebin El-Kom, Egypt

ABSTRACT

A computational study using BMK density functional theory and ab initio (CBS-QB3) methods has been performed to describe thermochemistry and kinetics of unimolecular decomposition reactions of 1,2-ethanediol monoacetate (2-hydroxyethylacetate) as a model biofuel. Formation of acetic acid and vinyl alcohol represents the most thermodynamically and kinetically preferable reaction until 400 K. After that, production of vinyl acetate becomes the main channel. The calculated enthalpies of formation for 1,2-ethanediol monoacetate and its radicals show a good agreement with the available experimental data.

Key words: 1,2-Ethanediol monoacetate, bifunctional, CBS-QB3, G3MP2, pyrolysis, biofuel.

Corresponding Author: El-Nahas, A. M.

INTRODUCTION

Over the last decades, scientists search for clean, efficient, and renewable energy sources to help in decreasing dependence on fossil fuels and reducing pollutions result from their combustion [1-4]. The use of renewable energy like solar cells, wind, hydropower and biofuels give good solutions for these problems [5-6]. Biofuels, fuels derived from biomass, [7-9] represent one of the most cost-effective energy resources when it is produced from non-edible crops or food residues. Biofuels can be used for different purposes in energy conversion, including transport, aviation, electricity generation...etc. Bioethanol is now one of the most common and abundant biofuels [10-12]. Ethanol is used more than methanol because it is considerably cleaner, less toxic and less corrosive [13]. Also there are n-butanol [14], 2-butanol [15], isobutanol [16] and propanol isomers [17] as examples of bioalcohols. Biodiesel fuel (a mixture of monoalkyl esters of long-chain fatty acids) is made from vegetable oils or animal fats [18]. It can be used without engine modification by its own or as a blend with petroleum diesel [19]. Biodiesel can be easily synthesized by transesterification of vegetable oils.

Bifunctional biofuels, compounds with two functional groups, are expected to enhance thermochemical properties of aliphatic esters by improving the properties of biofuel such as energy content, flash point and low vapor pressure compared to butanol isomers in addition to their miscibility in petroleum oils [20-24]. Starting from ethylene glycol one can obtain bifunctional biofuels such as 1,2-ethanediol monoacetate (2-hydroxyethylacetate) as an example of alcoholic ester biofuel [23]. It has also been determined that 1,2-ethanediol monoacetate is a very

promising candidate as an oxygenating additive to diesel fuels [23]. Using hydroxyl esters as bifunctional biofuels is expected to increase with the feasibility of their production from biomass. Ethylene glycol was obtained previously from biomass [25]. It has been reported that ethylene glycol monoacetate could be prepared from ethylene glycol in acetic acid solution containing LiNO₃ and Pd(OAc)₂ [26]. This alcoholic ester has boiling point of 187-189 °C, flash point of 102 °C and is stable under ordinary conditions.[27]. Verevkin et al. [23] conducted experimental and computational studies on 1,2-ethanediol monoacetate to determine thermochemical properties of biodiesel model. In this work, we are going to use density functional theory (DFT) and ab initio CBS-QB3 methods to study the thermochemistry and kinetics of the thermal decomposition of 2-hydroxyethylacetate (alcoholic ester) as a model biofuel.

COMPUTATIONAL DETAILS.

All electronic structure calculations have been performed with the Gaussian09w program [28]. Geometry optimization for 1,2-ethanediol monoacetate conformers has been done at G3MP2 [23] while geometry optimization and vibrational frequency calculations for 1,2-ethanediol monoacetate, its decomposition products, and relevant transition states have been carried out using the BMK density functional theory with the 6-31+G(d, p) basis sets [29]. The search for the transition states for unimolecular dissociation of the investigated ester has been carried out using the eigenvalue-following (EF) optimization procedures as implemented in the Gaussian program. For each stationary point, vibrational frequency calculations have been conducted at the same level used for optimization to characterize its nature as a minimum (positive frequencies) or transition state (only one negative frequency) and to correct the energies for zero-point and thermal contributions at 298 K. The vibrational modes were examined using the ChemCraft application to verify the existence of the transition states [30]. In addition, the complete basis set CBS-QB3 multi-level ab initio method was used for more accurate energies at low computational cost compared to more expensive ab initio procedures [31-32]. The kinetic parameters for different channels of 1,2-ethanediol monoacetate pyrolysis were determined over wide range of temperature using Kisthelp program [33].

The gas phase enthalpies of formation, $\Delta H_f^0(298)$ at a standard state of 1 atm for any molecule M containing n atoms was calculated as follows [34]:

$$\Delta H_{f\text{gas}}^0(M) = E_e(M) + ZPE(M) + [H_{298}(M) - H_0(M)] - \sum_i^{\text{atoms}} \{E_e(X_i) + [H_{298}(X_i) - H_0(X_i)]\} + \sum_i^{\text{atoms}} \Delta H_{f\text{gas}}^0(X_i)$$

Where $E_e(M)$ is the electronic energy of the molecule calculated at the chosen level of theory, ZPE is the zero-point energy of the molecule, $[H_{298}(M) - H_0(M)]$ is a thermal correction to the enthalpy obtained by means of simple Gibbs statistical mechanics, $E_e(X_i)$ is the electronic energy of the ith atom X calculated using the same technique. Enthalpies of formation for 1,2 ethanediol monoacetate , and the compounds formed through its decomposition were calculated using atomization approach (at CBS-QB3) and the results obtained compared with a viable experimental values, the comparison shows a good agreement with maximum deviation ± 2 kcal/mol, the obtained results gives a confidence in determination other unknown species.

RESULT AND DISCUSSION

Figure 1 displays optimized structures of four conformers of 1,2-ethanediol monoacetate calculated using G3MP2 [23]. It was found that the M3 conformer is the most stable isomer due to the presence of intramolecular hydrogen bond that is stronger than that one formed in M2 as reflected in the distance between the hydrogen of the hydroxyl group and the oxygen of the carbonyl group of 2.019 Å in M3 compared to 2.457 Å in M2. Relative energies of the four conformers are given in Table 1. From hereinafter, decomposition of M3 will be investigated.

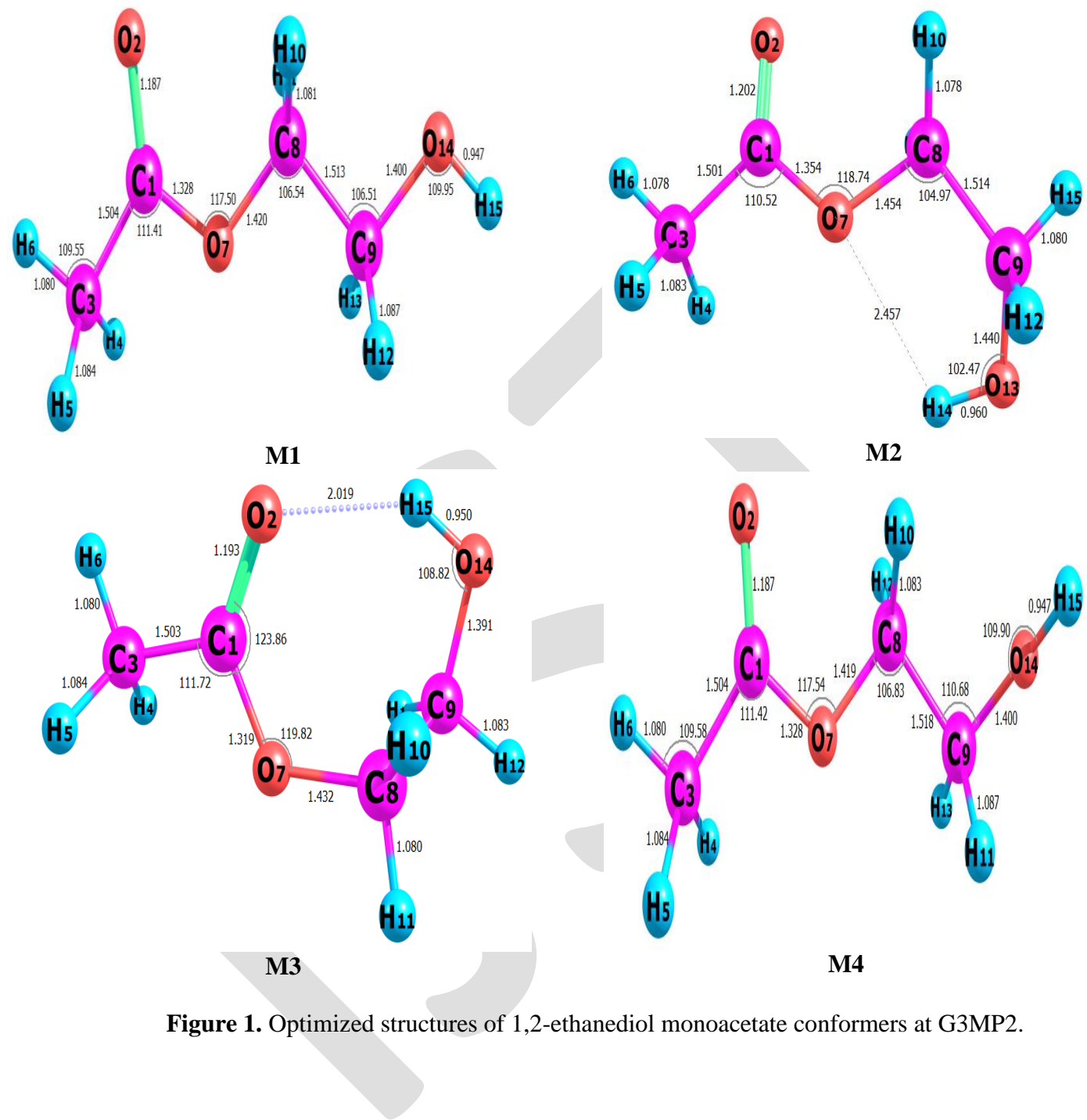


Figure 1. Optimized structures of 1,2-ethanediol monoacetate conformers at G3MP2.

Table 1. Relative energies for the four conformers of 1,2-ethanediol monoacetate (M) at G3MP2.

Conformer	Total energy (au)	Relative energy (kcal/mol)
M1	-382.369154	2.04
M2	-382.372372	0.02
M3	-382.372406	0.00
M4	-382.369192	2.02

Figure 2 illustrates bond dissociation energies (BDE) of 1,2-ethanediol monoacetate at CBS-QB3 composite method. The results indicate that the alcoholic O3-H bond is the strongest bond (107.2 kcal/mol) which close to published results [16] while C3-C4 (87.6 kcal/mol) is the weakest bond followed by C3-O (90.2 kcal/mol). The formation of CH₂OH via C3-C4 cleavage is the most preferable pathway on the potential energy surface of simple decomposition of 1,2-ethanediol monoacetate. For C-H bonds, the C4-H bond of 90.7 kcal/mol is the weakest one followed by C2-H (97.9 kcal/mol) with the C3-H bond is by 1.2 kcal/mol stronger than the C2-H bond. Among C-O bonds, the C1-O is the weakest (100.6 kcal/mol). BDEs presented in this work are comparable to those reported for other alcohols and esters [35-38].

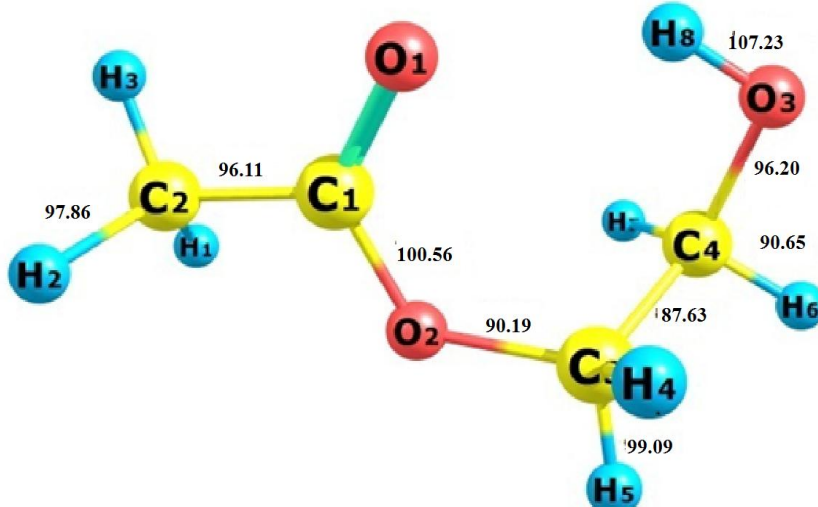


Figure 2. Bond dissociation energies (kcal/mol) of 1,2-diethanediol monoacetate M3 at CBS-QB3.

Enthalpies of formation for 1,2-ethanediol monoacetate and species produced from its decomposition were calculated using atomization approach at CBS-QB3 and are listed in Table 2. The calculated enthalpies of formation agree with the available experimental values and show a mean deviation of about ± 2 kcal/mol. This small deviation gives a confidence in the current computed enthalpies of formation for unknown species.

Pyrolysis of 1,2-ethanediol monoacetate can proceed either through complex fission reactions or by simple bond fission, we will concentrate here on the complex ones, among seven unimolecular complex reactions. Figure 3 displays the optimized structure of the most stable form of 1,2-ethanediol monoacetate model and the located transition states in the pathways of its unimolecular complex decomposition. The decomposition of 1,2-ethanediol monoacetate molecule can proceed through seven complex fission (barrier reactions) and nine simple bond scission reactions (barrierless reactions).

Complex bond fission reactions.

CH ₃ COOCH ₂ CH ₂ OH	→	CH ₂ CO	+ HOCH ₂ CH ₂ OH	R1
CH ₃ COOCH ₂ CH ₂ OH	→	CH ₃ COOH	+ CH ₂ =CHOH	R2
CH ₃ COOCH ₂ CH ₂ OH	→	CH ₃ COOCH ₃	+ HCHO	R3
CH ₃ COOCH ₂ CH ₂ OH	→	CH ₃ COOCH=CH ₂	+ H ₂ O	R4
CH ₃ COOCH ₂ CH ₂ OH	→	CH ₃ COOCH ₂ CHO	+ H ₂	R5
CH ₃ COOCH ₂ CH ₂ OH	→	CH ₂ =C(OH)OCH ₂ CH ₂ OH		R6
CH ₃ COOCH ₂ CH ₂ OH	→	CH ₃ COOCH ₂ CH	+ H ₂ O	R7

Simple bond fission reactions.

CH ₃ COOCH ₂ CH ₂ OH	→	CH ₂ COOCH ₂ CH ₂ OH	+ H·	R8
CH ₃ COOCH ₂ CH ₂ OH	→	CH ₃ COOC·HCH ₂ OH	+ H·	R9

$\text{CH}_3\text{COOCH}_2\text{CH}_2\text{OH}$	\rightarrow	$\text{CH}_3\text{COOCH}_2\text{C}\cdot\text{HOH}$	$+ \text{H}\cdot$	R10
$\text{CH}_3\text{COOCH}_2\text{CH}_2\text{OH}$	\rightarrow	$\text{CH}_3\text{COOCH}_2\text{CH}_2\text{O}\cdot$	$+ \text{H}\cdot$	R11
$\text{CH}_3\text{COOCH}_2\text{CH}_2\text{OH}$	\rightarrow	$\text{C}\cdot\text{OOCH}_2\text{CH}_2\text{OH}$	$+ \text{CH}_3$	R12
$\text{CH}_3\text{COOCH}_2\text{CH}_2\text{OH}$	\rightarrow	$\text{O}\cdot\text{CH}_2\text{CH}_2\text{OH}$	$+ \text{CH}_3\text{CO}\cdot$	R13
$\text{CH}_3\text{COOCH}_2\text{CH}_2\text{OH}$	\rightarrow	$\text{CH}_3\text{COO}\cdot$	$+ \text{CH}_2\text{CH}_2\text{OH}$	R14
$\text{CH}_3\text{COOCH}_2\text{CH}_2\text{OH}$	\rightarrow	$\text{CH}_3\text{COOC}\cdot\text{H}_2$	$+ \text{CH}_2\text{OH}$	R15
$\text{CH}_3\text{COOCH}_2\text{CH}_2\text{OH}$	\rightarrow	$\text{CH}_3\text{COOCH}_2\text{C}\cdot\text{H}_2$	$+ \text{O}\cdot\text{H}$	R16

Table 2. Enthalpies of formation ($(\Delta H^\circ_f, \text{kcal/mol})$) for 1,2-ethanediol monoacetate and its relevant species calculated using atomization energy approach at CBS-QB3.

Species	ΔH°_f	Exp.	Ref.
$\text{CH}_3\text{COOCH}_2\text{CH}_2\text{OH}$	-144.86	-142.37	[23]
$\text{HOCH}_2\text{CH}_2\text{OH}$	-94.76	-92.57	[39]
CH_3COOH	-104.32	-104.71	[40]
$\text{CH}_2=\text{CHOH}$	-28.65	-30.57	[41]
HCHO	-27.33	-26.05 ± 0.43	[42]
$\text{CH}_3\text{COOCH}_3$	-100.05	-98.83 ± 0.29	[43]
$\text{CH}_3\text{COOCH}=\text{CH}_2$	-74.03		
H_2O	-58.20	-57.8 ± 0.01	[44]
$\text{CH}_3\text{COOCH}_2\text{CHO}$	-121.73		
$\text{CH}_2\text{COHOCH}_2\text{CH}_2\text{OH}$	-115.12		
$\text{CH}_2\text{COOCH}_2\text{CH}_2\text{OH}$	-97.92		
$\text{CH}_3\text{COOC}\cdot\text{HCH}_2\text{OH}$	-96.69		
$\text{CH}_3\text{COOCH}_2\text{C}\cdot\text{HOH}$	-105.13		
$\text{CH}_3\text{COOCH}_2\text{CH}_2\text{O}\cdot$	-88.54		
CH_3	35.47	34.82	[45-46]
$\text{COOCH}_2\text{CH}_2\text{OH}$	-83.03		
$\text{CH}_3\text{C}\cdot\text{O}$	-2.50	-2.46	[47]
$\text{O}\cdot\text{CH}_2\text{CH}_2\text{OH}$	-40.61		
$\text{CH}_3\text{COO}\cdot$	-47.34		
$\text{CH}_2\text{CH}_2\text{OH}$	-6.15	-5.53	[48]
$\text{CH}_3\text{COOC}\cdot\text{H}_2$	-51.93		
CH_2OH	-4.11	-4.09 ± 0.81	[49]
$\text{CH}_3\text{COOCH}_2\text{C}\cdot\text{H}_2$	-56.29		
$\text{O}\cdot\text{H}$	8.82	8.91	[50]
CH_2CO	-11.71	-11.85 ± 0.21	[51]

Potential energy diagram ($(\Delta E_0, \text{kcal/mol})$) for complex unimolecular decomposition of 1,2-ethanediol monoacetate at BMK 6-31+G(d,p) and CBS-QB3 is depicted in Figure 4 [52]. All of the investigated channels are endothermic and the degree of endothermicity depends of the type of reaction. An inspection of Figure 4 indicates that the formation of acetic acid and vinyl alcohol is the most thermodynamically and kinetically favored reaction

on the potential energy surface (PES) of the complex decomposition of 1,2-ethanediol monoacetate. This channel has the lowest energy barrier ($\Delta E^* = 70.1$ kcal/mol at CBS-QB3) and it is least endothermic path ($\Delta E_0 = 12.5$ kcal/mol). The results obtained from BMK/6-31+G (d, p) are in a good agreement with those calculated using CBS-QB3 (deviation between 0.2-2.0 kcal/mol). In the following section, unless noted otherwise, all discussion will be done at the CBS-QB3 method.

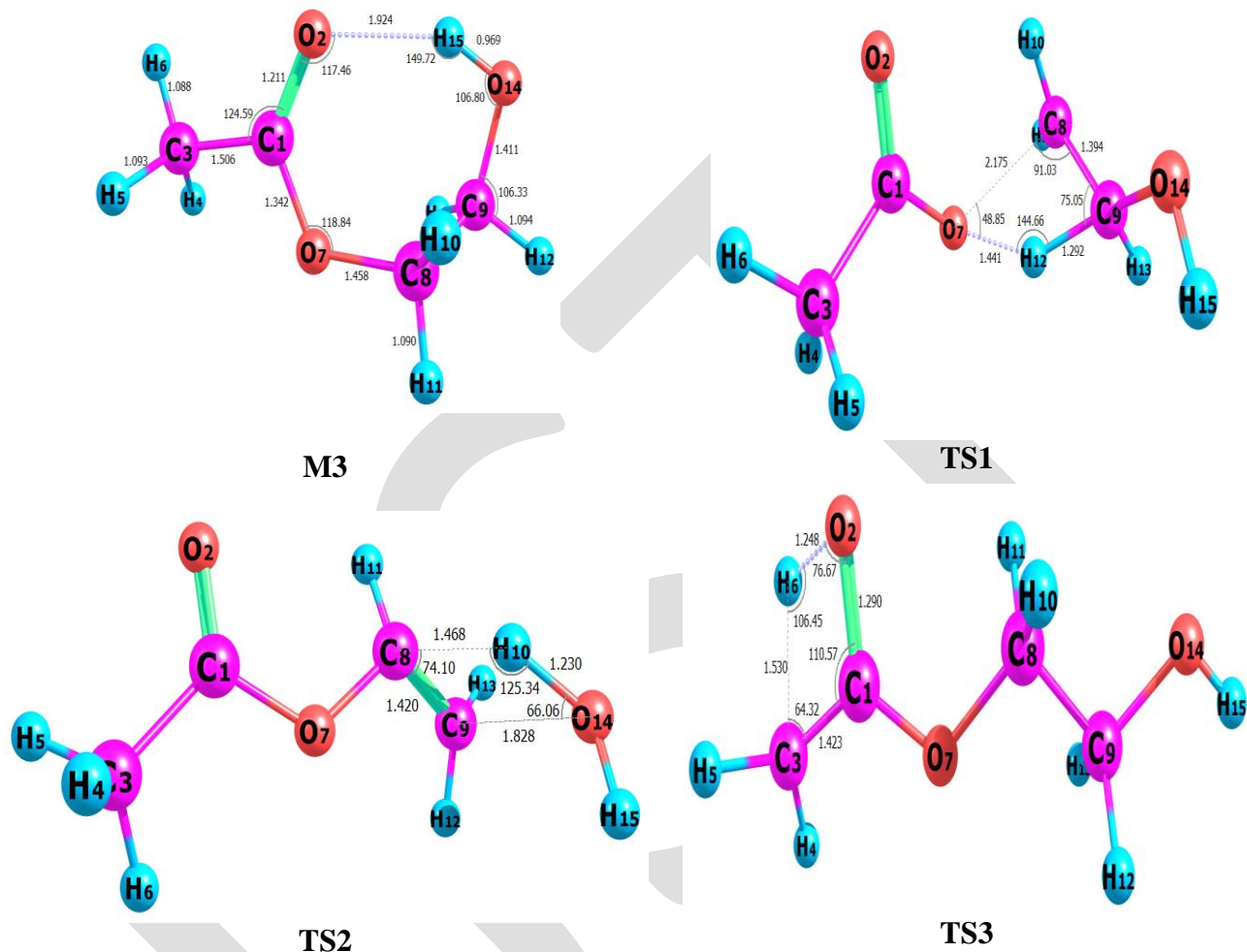


Figure 3. Optimized structures of 1,2-ethanediol monoacetate (which conformer,M3 or other) and transition states for its thermal degradation at CBS-QB3.

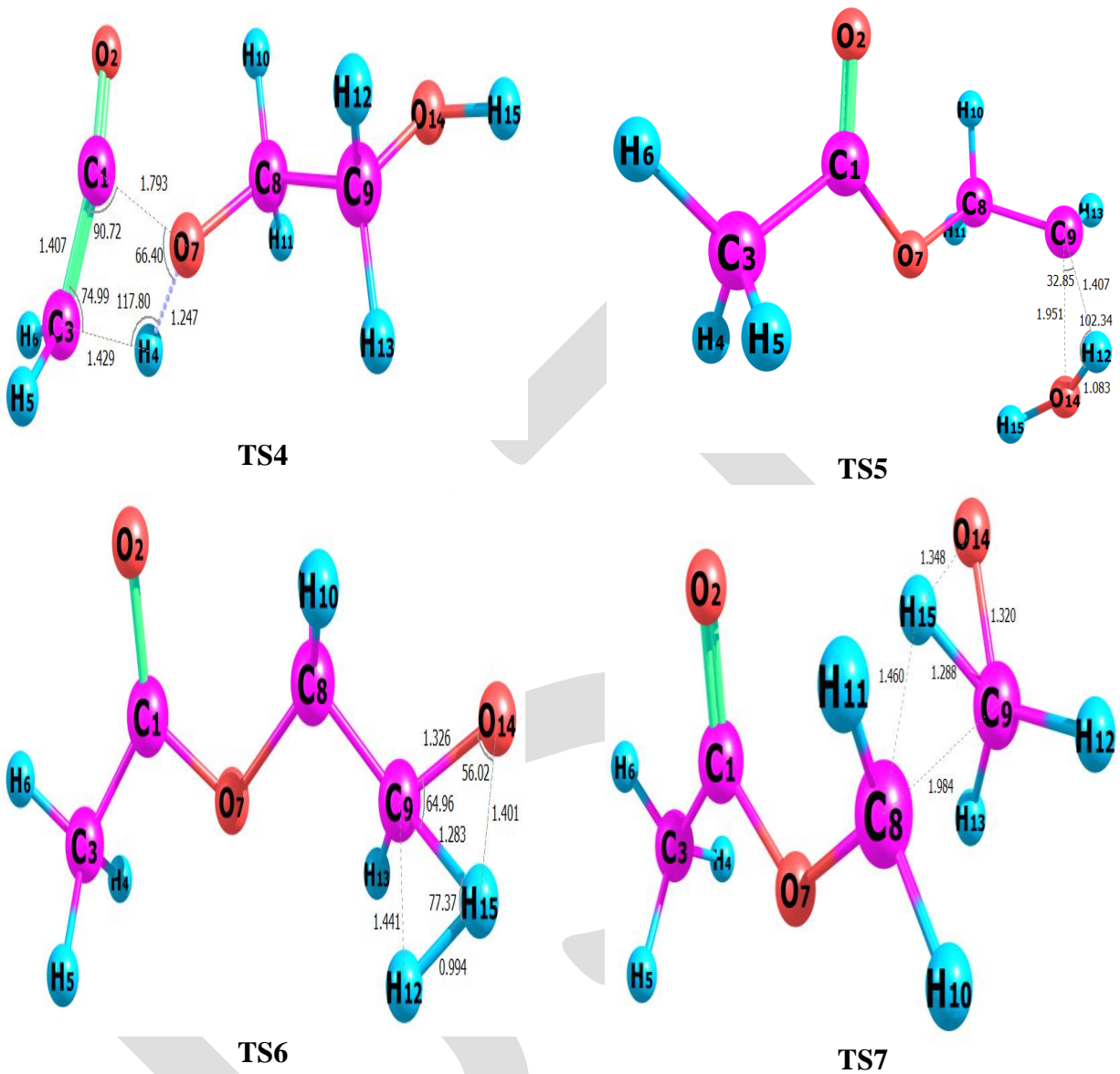


Figure 3. Continued

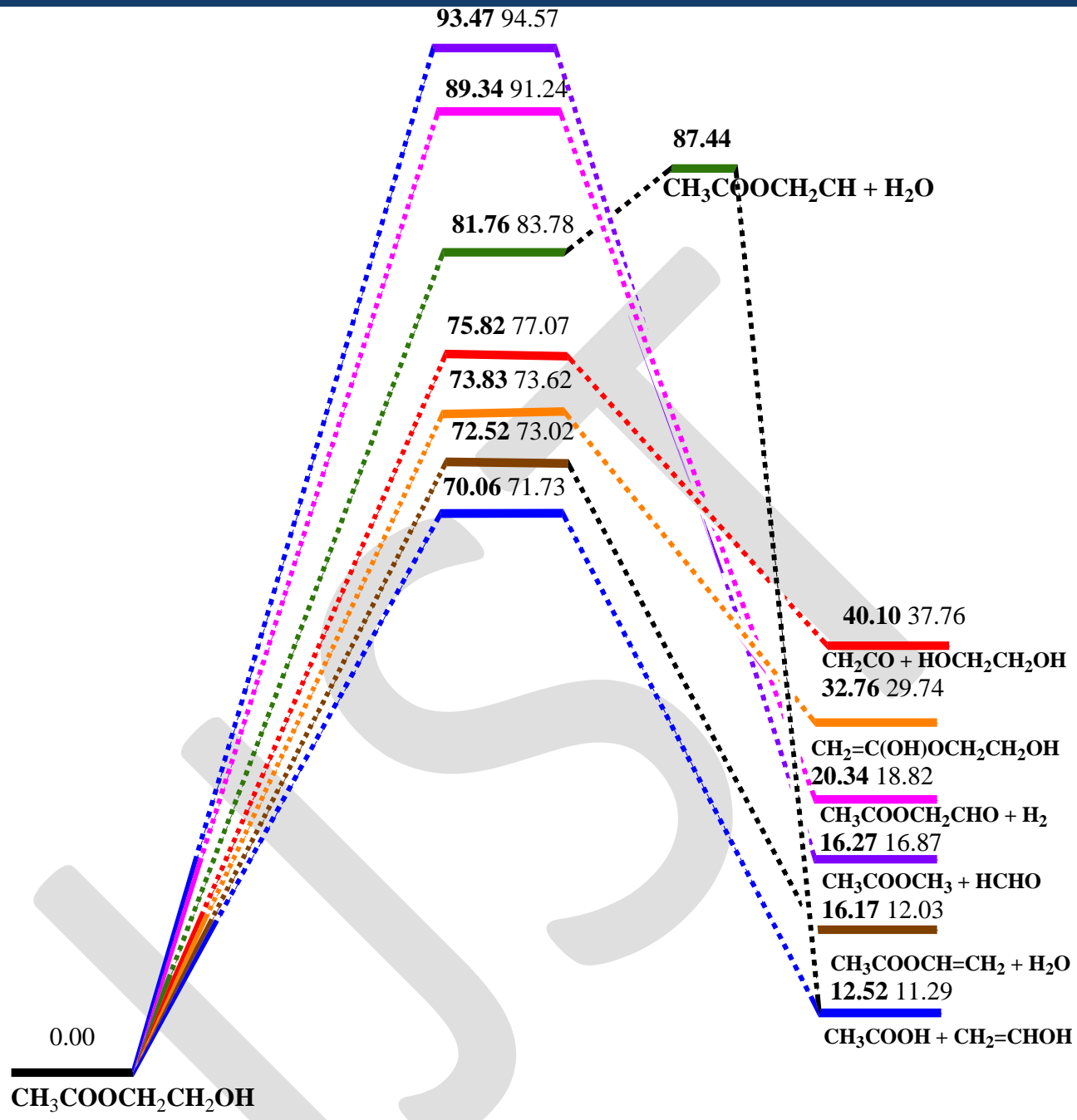


Figure 4. Potential energy diagram for unimolecular thermal decomposition of 1,2-ethanediol monoacetate (ΔE_0 , kcal/mol) at CBS-QB3 (bold) and BMK 6-31+G(d,p) (italic).

Table 3 presents branching ratios of complex decomposition pathways of 1,2-ethanediol monoacetate in the temperature range 200-2000 K. The formation of ethylene glycol and ketene (ethenone) contributes about 7% to the pyrolysis process at temperature over 1500 K. However, at temperature less than 400 K the dominated reaction is 1,5 hydrogen transfer that leads to the formation of acetic acid and vinyl alcohol while 1,2 water elimination reaction that gives vinyl acetate and water becomes the main channel at temperature above 500 K. The formation of dimethyl ester and formaldehyde in addition to the elimination of hydrogen molecule has a less contribution in a temperature range 200-2000 K. Figure 5 shows Arrhenius plots for the seven investigated

complex decomposition reactions of 1,2-ethanediol monoacetate over 200-2000 K, while Table 4 collects the corresponding kinetic parameters. When a reaction of higher activation energy predominates, this means that the frequency/collision factor (A) controls the reaction. The frequency factor is directly proportional to entropy. This is clear when comparing reactions 2 and 4 as well as reactions 1, 6, and 7. Reaction 5 that forms aldehydic ester has almost no contribution overall the investigated temperature range.

Table 3. Branching ratio (Γ) of pathways R₁, R₂, R₃, R₄, R₅, R₆ and R₇ in the overall reaction of the thermal decomposition of 1,2-ethanediol monoacetate.

Reaction/Temp	Γ_{R1}	Γ_{R2}	Γ_{R3}	Γ_{R4}	Γ_{R5}	Γ_{R6}	Γ_{R7}
200	0.00	84.83	0.00	15.10	0.00	0.07	0.00
298	0.04	67.22	0.00	32.23	0.00	0.50	0.00
300	0.05	66.91	0.00	32.53	0.00	0.52	0.00
400	0.26	54.10	0.00	44.46	0.00	1.18	0.00
500	0.70	45.51	0.00	52.00	0.00	1.806	0.00
600	1.31	39.56	0.00	56.85	0.00	2.26	0.02
700	2.03	35.24	0.00	60.06	0.00	2.60	0.08
800	2.78	31.97	0.00	62.23	0.00	2.83	0.20
900	3.52	29.40	0.00	63.69	0.00	2.99	0.41
1000	4.23	27.31	0.00	64.65	0.01	3.09	0.72
1100	4.89	25.58	0.00	65.23	0.01	3.16	1.13
1200	5.48	24.11	0.01	65.53	0.03	3.20	1.65
1300	6.02	22.84	0.01	65.61	0.04	3.22	2.26
1400	6.50	21.72	0.03	65.51	0.07	3.23	2.94
1500	6.93	20.74	0.04	65.28	0.10	3.23	3.69
1600	7.30	19.86	0.06	64.94	0.14	3.21	4.49
1700	7.63	19.06	0.09	64.52	0.19	3.19	5.31
1800	7.93	18.34	0.12	64.03	0.24	3.17	6.16
1900	8.18	17.69	0.16	63.50	0.31	3.14	7.03
2000	8.40	17.09	0.21	62.93	0.38	3.11	7.89

Table 4. Kinetic parameters for the reactions R₁, R₂, R₃, R₄, R₅, R₆ and R₇ over the temperature range 200-2000 K at (CBS-QB3).

Reaction	E _a kcal/mol	A(s ⁻¹)
R ₁	76.07	2.38E+14
R ₂	71.48	1.53E+14
R ₃	93.49	4.94E+14
R ₄	72.84	7.36E+14
R ₅	89.37	3.09E+14
R ₆	73.79	5.39E+13
R ₇	82.66	1.11E+15

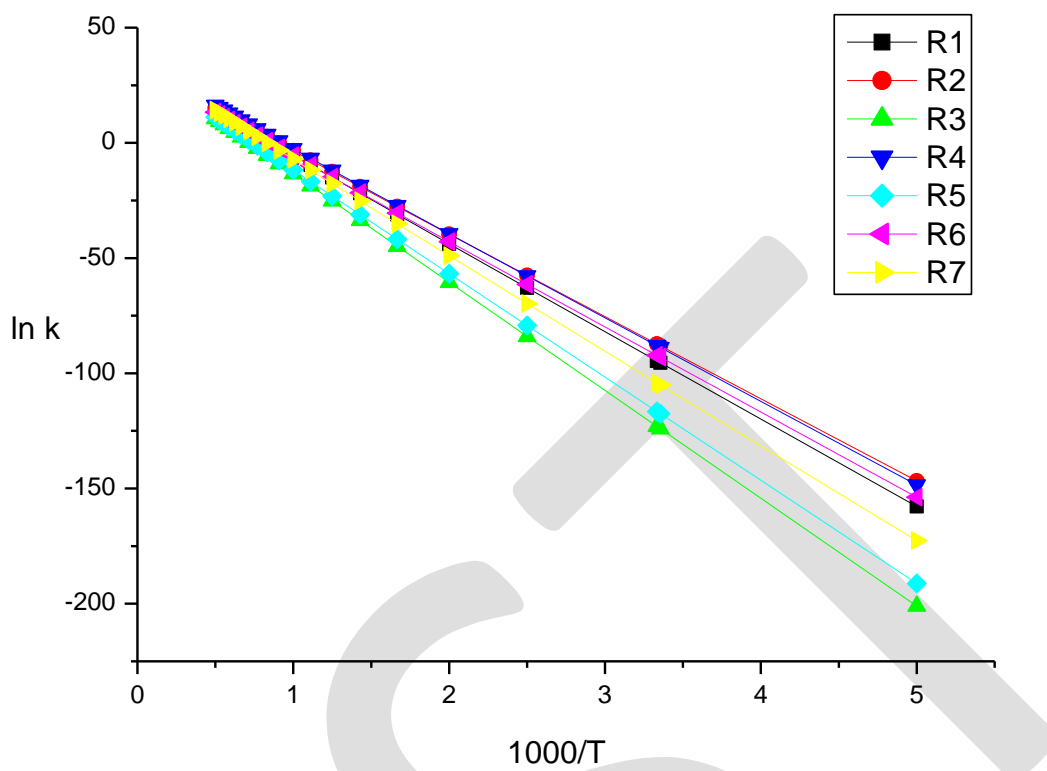


Figure 5. Arrhenius plots for 1,2-ethanediol monoacetate pyrolysis through decomposition reactions R1, R2, R3, R4, R5, R6 and R7 over temperature range (200-2000K).

CONCLUSION

Using the density functional theory at BMK6-31+G(d,p) and ab initio CBS-QB3 procedures, this work describes thermochemistry and kinetics of the decomposition of 1,2-ethanediol monoacetate (2-hydroxyethylacetate) as a bioalcoholic ester as a model biofuel. The obtained results can be summarized as follows:

1. The calculated enthalpies of formation for 1,2-ethanediol monoacetate and its radicals show a good agreement with the available experimental data.
2. 1,2-Ethanediol monoacetate could function as a biofuel because of its physical properties and decomposition pattern that is comparable to alcohols and esters.
3. Formation of acetic acid and vinyl alcohol represents the most thermodynamically and kinetically preferable reaction until 400 K. After that, production of vinyl acetate becomes the main channel.

REFERENCES

- [1] S. Shafiee, E. Topal, When will fossil fuel reserves be diminished?, *Energy Policy* 37 (2009) 181-189.
- [2] A. S. Alshehrya, M. Belloumia, Energy consumption, carbon dioxide emissions and economic growth: the case of Saudi Arabia, *Renew. Sustain. Energy Rev.* 41 (2015) 237-247.
- [3] D. E. Pataki, P. C. Emmi, C. B. Forster, J. I. Mills, E. R. Pardyjak, T. R. Peterson, J. D. Thompson, E. D. Murphy, An integrated approach to improving fossil fuel emissions scenarios with urban ecosystem studies, *Ecological Complexity* 6 (2009) 1-14.

- [4] G. R. Van der Werf, D. C. Morton, R. S. DeFries, J. G. J. Olivier, P. S. Kasibhatla, R. B. Jackson, G. J. Collatz, J. T. Randerson, CO₂ emissions from forest loss, *Nature Geosci.* 2 (2009) 737 – 738.
- [5] C. de Fraiture, M. Giordano, Y. Liao, Biofuels and implications for agricultural water use: blue impacts of green energy, *water policy* 10 supplement 1 (2008) 67-81.
- [6] G. Sorda, M. Banse, C. kemfert, An overview of biofuel policies across the world, *Energy policy* 38 (2010) 6977-6988.
- [7] H. B. Goyal, D. Seal, R. C. Saxena, Bio-fuels from thermochemical conversion of renewable resources: A review 12 (2008) 504-517.
- [8] P. J. Crutzen, M. O. Andreae, Biomass Burning in the Tropics: Impact on Atmospheric Chemistry and Biogeochemical Cycles, book 50 (2016) 165-188
- [9] A. Trubetskaya, P. A. Jensen, A. D. Jensen, A. D. G. Llamas, K. Umeki, D. Gardini, J. Kling, R. B. Bates, P, Glarborg, Effects of several types of biomass fuels on the yield, nanostructure and reactivity of soot from fast pyrolysis at high temperatures, *App. Energy* 171 (2016) 468-482.
- [10] A. Demirbas, Biofuels sources, biofuel policy, biofuel economy and global biofuel projections, *Energy Convers. Manage.* 8 (2008) 2106–2116.
- [11] H. Zabed , J. N. Sahu, A. Suely, A. N. Boyce, G. Faruq, Bioethanol production from renewable sources: Current perspectives and technological progress, *Renew. Sustain. Energy Rev.* 71 (2017) 475–501.
- [12] M. F. Demirbas, M. Balat, H. Balat, Biowastes-to-biofuels, *Energy Convers. Manage.* 52 (2011) 1815–1828.
- [13] M. Balat, H. Balat, C. Oz, Progress in bioethanol processing, *J. Proc. Combust. Inst.* 34 (2008) 551-573.
- [14] T. L. Richard, Challenges in scaling up biofuels infrastructure, *Science*, 329 (2010) 793-796.
- [15] R. L. Wingad, E. J. E. Bergstrom, M. Everett, K. J. Pellow, D. F. Wass, Catalytic conversion of methanol/ethanol to isobutanol – a highly selective route to an advanced biofuel, *Chem. Comm.* 52 (2016) 5202-5204.
- [16] A. M. El-Nahas, A. H. Mangood, A. B. El-Meleigy, A computational study on the structures and energetics of isobutanol pyrolysis, *Comp. Theor. Chem.* 997 (2012) 94–102.
- [17] T. Kasper, P. OBwald, U. Struckmeier, K. K. Höinghaus, C. A. Taatjes, J. Wang, T. A. Cool, M. E. Law, A. Morel, P. R. Westmoreland, Combustion chemistry of the propanol isomers - investigated by electron ionization and VUV-photoionization molecular-beam mass spectrometry, *Combust. Flame* 156 (2009) 1181–1201.
- [18] D. Lipkind, Y. Kapustin, P. Umnahanant, J. S. Chickos, The vaporization enthalpies and vapor pressures of a series of unsaturated fatty acid methyl esters by correlation gas chromatography, *Thermochim. Acta* 456 (2007) 94–101.
- [19] L. Wei, C. S. Cheung, Z. Ning, Influence of waste cooking oil biodiesel on combustion, unregulated gaseous emissions and particulate emissions of a direct-injection diesel engine, *Energy* 127 (2017) 175–185.
- [20] S. Thion, A. Zaras, M. Szori, P. Dagaut, Theoretical kinetic study for methyl levulinate oxidation by OH and CH₃ radicals and further unimolecular decomposition pathways, *Chem. Phys. Chem.*,17 (2015) 23384-23391.
- [21] X. Guo, J. Guan, B. Li, X. Wang, X. Mu, H. Liu, Conversion of biomass-derived sorbitol to glycols over carbon-materials supported Ru- based catalysts, *Sci. Rep.* 5 (2015) 16451-16460.
- [22] L. Ye, L. Zhage, F. Qi, Theoretical studies on the unimolecular decomposition of propanediols and glycerol, *Chem. Phys. Chem.*, 116 (2012) 4457-4465.
- [23] S. P. Verevkin, V. N. Emel'yanenko, A. V. Toktonov, A. S. Leolko, Thermochemical and Ab Initio Studies of Biodiesel Fuel Surrogates: 1,2,3-Propanetriol Triacetate, 1,2-Ethanediol Diacetate, and 1,2-Ethanediol Monoacetate, *Ind. Eng. Chem. Res.* 48 (2009) 7388–7399.
- [24] C. Y. Lin, J. C. Huang, An oxygenating additive for improving the performance and emission characteristics of marine diesel engines, *Ocean Engineering* 30 (2003) 1699–1715.
- [25] N. Ji, T. Zhang, M. Zheng, A. Wang, H. Wang, X. Wang, and J. G. Chen. Direct Catalytic Conversion of Cellulose into Ethylene Glycol Using Nickel-Promoted Tungsten Carbide Catalysts, *Angew. Chem. Int. Ed.* 47 (2008) 8510–8513.

- [26] N. Kuznetsova, V. A. Likhobov, M. A. Fedotov, Y. I. Yermakov, The mechanism of formation of ethylene glycol monoacetate from ethylene in the system $\text{MeCO}_2\text{H} + \text{LiNO}_3 + \text{Pd}(\text{OAc})_2$, J. Am. Chem. Soc, Chem. Comm. 17 (1982) 973-974.
- [27] R. P. Pohanish, S. A. Greene, Wiley Guide to Chemical Incompatibilities, book (2009) 468-469.
- [28] M. J. Frisch, G. W. Trucks, H. B. Schlegel, G. E. Scuseria, M. A. Robb, J. R. Cheeseman, G. Scalmani, V. Barone, B. Mennucci, G. A. Petersson, H. Nakatsuji, M. Caricato, X. Li, H. P. Hratchian, A. F. Izmaylov, J. Bloino, G. Zheng, J. L. Sonnenberg, M. Hada, M. Ehara, K. Toyota, R. Fukuda, J. Hasegawa, M. Ishida, T. Nakajima, Y. Honda, O. Kitao, H. Nakai, T. Vreven, J. A. Montgomery Jr., J. E. Peralta, F. Ogliaro, M. Bearpark, J. J. Heyd, E. Brothers, K. N. Kudin, V. N. Staroverov, R. Kobayashi, J. Normand, K. Raghavachari, A. Rendell, J. C. Burant, S. S. Iyengar, J. Tomasi, M. Cossi, N. Rega, J. M. Millam, M. Klene, J. E. Knox, J. B. Cross, V. Bakken, C. Adamo, J. Jaramillo, R. Gomperts, R. E. Stratmann, O. Yazyev, A.J. Austin, R. Cammi, C. Pomelli, J. W. Ochterski, R. L. Martin, K. Morokuma, V. G. Zakrzewski, G. A. Voth, P. Salvador, J. J. Dannenberg, S. Dapprich, A. D. Daniels, O. Farkas, J. B. Foresman, J. V. Ortiz, J. Cioslowski, D. J. Fox, Gaussian 09; Gaussian, Inc.: Wallingford, CT, 2009.
- [29] A. D. Boese, J. M. L. Martin, Development of density functionals for thermochemical kinetics, J. Phys. Chem. A 121 (2004) 3405-3416.
- [30] G. A. Zhurko, Chemcraft V1.6. <http://www.chemcraftptrog.com>.
- [31] J. A. Montgomery Jr., M. J. Frisch, J. W. Ochterski, G. A. Petersson, A complete basis set model chemistry . VII. Use of density functional geometries and frequencies, J. Chem. Phys. 11 (1999) 2822-2827.
- [32] J. A. Montgomery Jr., M. J. Frisch, J. W. Ochterski, G. A. Petersson, A complete basis set model chemistry . VII. Use of the minimum population localization method, J. Chem. Phys. 11 (2000) 6532-6542.
- [33] S. Canneaux, F. Bohr, E. Henon, KiSThelP: a program to predict thermodynamic properties and rate constants from quantum chemistry results, J. Comput. Chem. 35 (2014) 82-93.
- [34] H. Y. Afeefy, J. F. Liebman, S. E. Stein, P. J. Linstrom, W. G. Mallard, Neutral Thermochemical Data in Nist Chemistry WebBook, NIST Standard Reference Database Number 69, June 2005, National Institute of Standards and Technology, Gaithersburg, MD 20899, p. 106. <http://webbook.nist.gov> (retrieved 31.10.08).
- [35] P. J. Gardner, K. S. Hussain, The standard enthalpies of formation of some aliphatic diols, J. Chem. Thermodynam. 4 (1972) 819-827.
- [36] Y. Zhang, L. Boehman, Oxidation of 1-butanol and a mixture of n-heptane/1-butanol in a motored engine, Combust. Flame 157 (2010) 1816-1824.
- [37] M. V. Johnson, S. S. Goldsborough, Z. Serinyel, P. O'Toole, E. Larkin, G. O'Malley, H. Curran, A Shock Tube Study of n- and iso-Propanol Ignition, J. Energy Fuels 23 (2009) 5886–5898.
- [38] A. Frassoldati, A. Cuoci, T. Faravelli, U. Niemann, E. Ranzi, R. Seiser, K. Seshadri; An experimental and kinetic modeling study of n-propanol and iso-propanol combustion; Combust. and Flame 157 (2010) 2-16
- [39] A. M. El-Nahas, L. A. Heikal, A. H. Mangood, E. E. El-Shereefy, Structures and Energetics of Unimolecular Thermal Degradation of Isopropyl Butanoate as a Model Biofuel: Density Functional Theory and Ab Initio Studies, J. Phys. Chem. 114 (2010) 7996–8002
- [40] W. V. Steele , R. D. Chirico , A. B. Cowell , S. E. Knipmeyer , A. Nguyen, Thermodynamic Properties and Ideal-Gas Enthalpies of Formation for 2-Aminoisobutyric Acid (2-Methylalanine), Acetic Acid, (Z)-5-Ethylidene-2-norbornene, Mesityl Oxide (4-Methyl-3-penten-2-one), 4-Methylpent-1-ene, 2,2'-Bis(phenylthio)propane, and Glycidyl Phenyl Ether (1,2-Epoxy-3-phenoxypropane), J. Chem. Eng. Data 42 (1997) 1053–1066.
- [41] F. Turecek, Z. Havlas, Thermochemistry of unstable enols: the O-(Cd)(H) group equivalent, J. Org. Chem., 51 (1986) 4066-4067.
- [42] G. da Silva, J.W. Bozzelli, N. Sebbar, and H. Bockhorn, Thermodynamic and ab initio analysis of the controversial enthalpy of formation of formaldehyde, Chem. Phys. Chem. 7 (2006) 1119–1126.

- [43] S. P. Verevkin, H. D. Beckhaus, R. S. Belen'kaja, K. Rakus, C. Ruchardt, Geminale substituent effect. Part 9. Standard enthalpies of formation and strain free increments of branched esters and ethers, *Thermochim. Acta* 279 (1996) 47–64.
- [44] J. D. Cox, D. D. Wagman, and V. A. Medvedev, CODATA Key Values for Thermodynamics, Hemisphere Publishing Corp., New York, 1984. p.1.
- [45] W. Tsang, J. A. M. Simoes, A. Greenberg, J. F. Lieberman, Energetics of Organic Free Radicals, Blackie Academic and Professional, London, 1996. pp. 22-58.
- [46] M. W. Chase Jr., NIST-JANAF Thermochemical Tables, fourth ed., *J. Phys. Chem. Ref. Data*, Monograph 9 (1998) 1–1951.
- [47] B. Ruscic, J. E. Boggs, A. Burcat, A. G. Császár, et al., IUPAC critical evaluation of thermochemical properties of selected radicals, Part I , *J. Phys. Chem. Ref. Data* 34 (2005) 573-656.
- [48] L. A. Curtiss, D. J. Lucas, and J. A. Pople, Energies of C_2H_5O and $C_2H_5O^+$ isomers, *J. Chem. Phys.* 102 (1995) 3292-3300.
- [49] P. M. Mayer, M. N. Glukhovtsev, J. W. Gauld, L. Radom, The effects of protonation on the structure, stability and thermochemistry of carbon centered organic radicals, *J. Am. Chem. Soc.*, 119 (1997) 12889–12895.
- [50] A. Burcat, B. Ruscic, Ideal Gas Thermochemical Database with updates from Active Thermochemical Tables, Wiley, York, 10 August 2007, <ftp://ftp.technion.ac.il/pub/supported/aetdd/thermo dynamics>.
- [51] B. Ruscic, M. Litorja, R. L. Asher, Ionization Energy of Methylene Revisited: Improved Values for the Enthalpy of Formation of CH_2 and the Bond Dissociation Energy of CH_3 via Simultaneous Solution of the Local Thermochemical Network, *J. Phys. Chem. A* 103 (1999) 8625–8633.
- [52] J.P. Merrick, D. Moran, L. Radom, An evaluation of harmonic vibrational frequency scale factors, *J. Phys. Chem. A* 111 (2007) 11683–11700.